Polymer Chemistry

Mechanically Robust and Reprocessable Imine Exchange Networks from Modular Polyester Pre-Polymers

Journal:	*Polymer Chemistry*
Manuscript ID	PY-ART-12-2019-001957.R1
Article Type:	Paper
Date Submitted by the Author:	10-Feb-2020
Complete List of Authors:	Hillmyer, Marc; University of Minnesota, Chemistry Coates, Geoffrey; Cornell University, Chemistry and Chemical Biology Snyder, Rachel; Cornell University, Chemistry and Chemical Biology Parvulescu, Maria; Cornell University, Chemistry and Chemical Biology De Hoe, Guilhem; University of Minnesota Twin Cities, Chemistry Lidston, Claire; Cornell University, Chemistry and Chemical Biology

ARTICLE

Mechanically Robust and Reprocessable Imine Exchange Networks from Modular Polyester Pre-Polymers

Received 00th January 20xx,
Accepted 00th January 20xx

DOI: 10.1039/x0xx00000x

Rachel L. Snyder,[†,a] Claire A. L. Lidston,[†,a] Guilhem X. De Hoe,[‡,b,c] Maria J. S. Parvulescu,[‡,a,d] Marc A. Hillmyer,[b,*] and Geoffrey W. Coates[a,*]

Covalent adaptable networks (CANs) containing reversible cross-links impart recyclability to thermoset materials without sacrificing their desirable properties (*e.g.* high tensile strength and solvent resistance). In addition to thermal recycling, the sustainability of these materials may be further improved by incorporating bio-sourced monomers or by enabling alternate end-of-life fates, such as biodegradation or recovery of starting materials. The alternating ring-opening copolymerisation of epoxides and cyclic anhydrides permits the modular synthesis of polyester pre-polymers that can then be cross-linked to form dynamic imine-linked networks. We report the synthesis and characterisation of five imine exchange polyester CANs with varied cross-linking densities and pre-polymer architectures. While the materials exhibit characteristic thermoset properties at service temperatures, differences in pre-polymer architecture produce distinct dynamic mechanical effects at elevated temperatures. The networks may be thermally reprocessed with full recovery of their tensile strength and cross-linking density, dissociated to pre-polymer, or hydrolytically degraded.

Introduction

Currently, the polymer community is focused on developing materials that are compatible with a sustainable future.[1–3] This goal requires consideration of not only how a material is sourced, but also how to extend its functional lifetime and promote eco-friendly end-of-life options. While permanently cross-linked thermosets offer high thermal and dimensional stability, they are classically non-recyclable and are consequently landfilled or incinerated.[4] Incorporating dynamic linkages into cross-linked polymers affords covalent adaptable networks (CANs) that can be reshaped and reprocessed.[3–11] CANs typically exhibit robust properties at service temperatures but flow upon thermal activation as their dynamic bonds exchange. While traditional thermosets must be processed via injection molding and solvent casting from monomers, CANs are amenable to bulk reprocessing via extrusion,[12] welding,[13] and 3D printing.[14] Furthermore, their mechanical properties and chemical integrity can be maintained over multiple reprocessing cycles, enabling recycling and extended functional lifetimes. Incorporating bio-sourced monomers and degradable backbone functionalities can further improve the sustainability of CANs.

Typically, CANs are categorized by their bond exchange mechanisms – associative or dissociative – which dictate the thermomechanical properties of the polymers before, during, and after reprocessing.[7,8] In associative networks (vitrimers), bond-breaking and bond-forming events occur simultaneously, typically through an associative exchange mechanism. In 2011, Leibler demonstrated associative exchange in a polymer network using catalysed transesterification between pendant hydroxyl groups and the polyester backbone.[12] Isodesmic exchange prevents decreases in cross-linking density, preserving the network's structural integrity during processing.[11,12] In contrast, dissociative networks contain dynamic linkages that first disconnect and then recombine with other partners. An early example of dissociative CANs was reported by Wudl et al. in 2002 wherein Diels-Alder chemistry between furans and maleimides afforded remouldable networks.[15] The viscosity of dissociative materials decreases rapidly as cross-links are cleaved, which can improve processability. However, the thermodynamic equilibrium between association/dissociation determines the cross-linking density, requiring precise thermal control to achieve consistent mechanical properties. Notably, "vitrimer-like" thermomechanical properties can be achieved in dissociative networks if the exchange equilibrium is shifted heavily towards association.[16]

Since the early reports by Wudl[15] and Leibler,[12] numerous dynamic chemistries have been successfully employed in cross-linked networks; however, these materials still face practical

[a] *Department of Chemistry and Chemical Biology, Baker Laboratory, Cornell University, Ithaca, New York 14853-1301, United States.*
[b] *Department of Chemistry, University of Minnesota, Minneapolis, Minnesota 55455-0431, United States.*
[c] Present address: Center for Molecular Engineering, Argonne National Laboratory, Lemont, Illinois 60439, United States.
[d] Present address: UES, Inc. Dayton, OH 45432, United States.
[†] These authors contributed equally to this work.
[‡] These authors contributed equally to this work.
Electronic Supplementary Information (ESI) available: synthetic procedures, experimental controls, supplementary characterisation including ^{1}H and ^{13}C NMR spectra, FT-IR spectra, GPC data, TGA data, DSC data, rheological data, tensile testing data, and dissolution data. See DOI: 10.1039/x0xx00000x

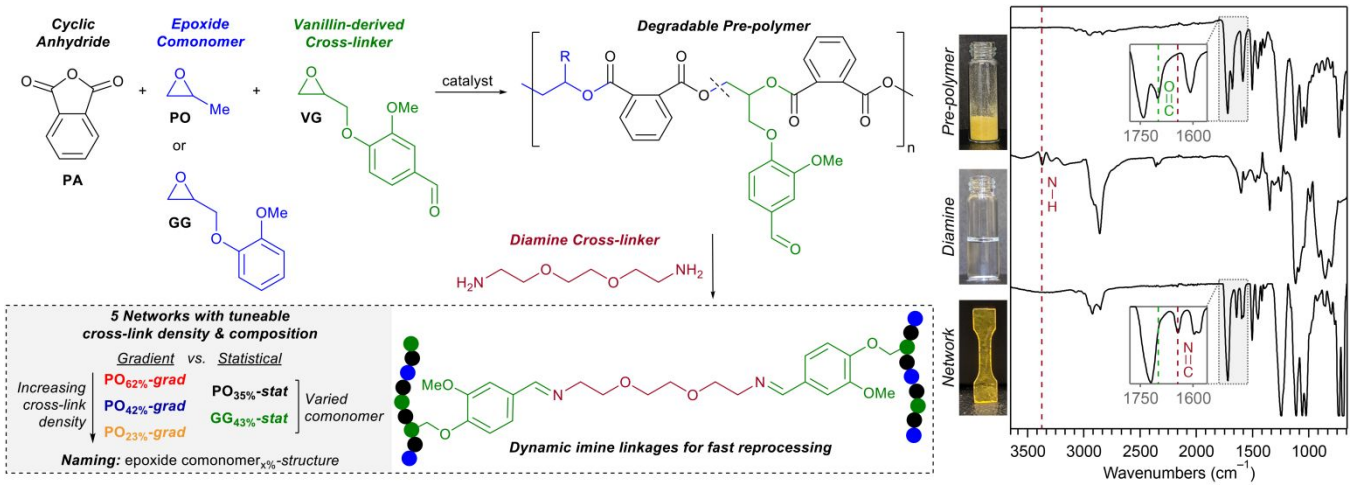

Fig 1 Ring-opening copolymerisation between cyclic anhydride, renewable cross-linker **VG,** and an epoxide comonomer gives polyester pre-polymers that can be cross-linked with a diamine to form dynamic imine-based covalent adaptive networks. The **VG** content and epoxide co-monomer can be tuned to give different cross-linking densities, and reaction conditions can be modified to achieve gradient or statistical pre-polymer architectures. The polymer naming convention is epoxide comonomer$_{x\%}$-*structure*, where the epoxide comonomer is either **PO** or **GG**, x% represents the percent incorporation of epoxide comonomer with respect to 100% **PA** incorporation, and terpolymer structure is gradient (*grad*) or statistical (*stat*). FT-IR spectra of the networks show complete consumption of aldehyde and amine from the starting materials and the appearance of an imine stretch peak.

challenges. Modularity through monomer design is often difficult, constraining potential applications due to inaccessible thermal and mechanical properties. Furthermore, relatively slow rates of both bond exchange and flow prompt extended reprocessing times at high temperatures. These intense conditions can lead to undesirable polymer degradation and prevent complete recovery of material properties after reprocessing.[17] As a result, many vitrimers employ catalysts to facilitate exchange at more practical temperatures, but these catalysts can be costly and may become deactivated or leach into the environment.[18,19] Therefore, developing thermally and mechanically robust CANs that exhibit fast exchange without exogenous catalyst is particularly desirable.

Vinylogous urethanes[20–22] and ureas,[23] hydroxyurethanes,[17] thiols,[24] disulfides,[25–27] silyl ethers,[28,29] dioxaborolanes,[30] boroxines,[31] and imines[32–42] have been incorporated in reprocessable networks without added catalyst. Of these, imine exchange is known to be particularly fast and robust under mild conditions, and the exchange dynamics can be controlled thermally, by water content, or with pH changes. In addition, imines can exchange via hydrolysis (dissociative), transimination (associative), or metathesis (associative).[43,44] Both aromatic and aliphatic imines have been incorporated into CANs that undergo fast reprocessing and exhibit good recovery of polymer properties over multiple cycles.[32–42] Taynton and Zhang *et al.* have described several polymer networks based on imine exchange and demonstrated the effects of varied monomer structure,[37,40] water content,[38] and carbon fiber reinforcement[39] on material properties. Several examples of self-healing, remoulding, and shape memory facilitated by imine dynamics have also been reported.[32,33,36,37,41,42]

While exchange reactions remain at the forefront of CAN research, cross-link density and uniformity have recently emerged as influential factors in the rheological properties of CANs. Sumerlin and Kalow demonstrated that pre-polymer structure (blocky versus statistical) influences the thermal and rheological properties of acrylic dynamic covalent networks with vinylogous urethane linkages.[45,46] The authors propose that microphase separation can isolate the dynamic linkages in the minority phase of the material, causing higher local cross-link concentrations in the blocky networks. These materials demonstrate similar stress relaxation times and Arrhenius activation energies; however, the blocky materials exhibit improved creep resistance. Leibler and coworkers have also proposed that non-uniform cross-linking caused by microphase separation could improve processability, as phase-separated chains may plasticize the networks at elevated temperatures.[47] Therefore, monomer structures, exchange chemistry, and network architecture must be considered in the design and characterization of novel CANs.

The alternating ring-opening copolymerisation (ROCOP) of epoxides and cyclic anhydrides provides a living, chain-growth approach to synthesize aliphatic and semi-aromatic polyesters from commercially available or readily synthesized monomer pairs.[48,49] However, ROCOP is often plagued by adventitious initiating species (e.g. H_2O), which limit the accessible molar masses and, consequently, polymer mechanical properties.[50–58] Nonetheless, polyesters are valuable commodity materials with potential for eco-friendly end-of-life options, such as hydrolytic degradation.[59–63] Epoxide/cyclic anhydride ROCOP remains an attractive platform for polyester synthesis due to its controlled chain-growth behavior and compatibility with bio-based monomers.[50,51,64] The Coates group recently reported ROCOP of a vanillin-derived epoxide (**VG**, Figure 1), wherein post-polymerisation functionalisation using an alkyl monoamine resulted in quantitative conversion of aldehyde to imine without cleavage of the polyester backbone.[58] We envisioned that low molar mass epoxide/cyclic anhydride polyesters containing pendant aldehydes from **VG** could react similarly with a diamine to form imine cross-linked networks with desirable mechanical properties.

Recently, a number of groups have incorporated **VG** and other lignin-derived monomers into dynamic imine networks that can be reshaped, welded, and reprocessed, or, alternatively, solubilized and degraded.[41,65–70] Yet to date, dynamic imine CANs incorporating **VG** have been exclusively synthesized via step-growth approaches from discrete small molecules. Epoxide/cyclic anhydride ROCOP is a highly modular chain-growth approach, allowing facile variation of pre-polymer composition and architecture through comonomer choice, stoichiometry, and reaction conditions. We propose using ROCOP to incorporate **VG**[71–73] into a polyester backbone with other fully or partially bio-sourced monomers (guaiacol glycidyl ether,[74–76] **GG**, and phthalic anhydride,[64,77,78] **PA**) or propylene oxide[79] (**PO**). Subsequent reaction with a diamine would install dynamic imine cross-links (Figure 1). While economically viable sourcing and "green" synthetic procedures still need to be optimized for bio-based monomers, they are potentially advantageous feedstocks as compared to commodity petrochemicals. More importantly, such polyester imine CANs may be recycled via multiple avenues, including direct thermal reprocessing, dissolution and recovery of pre-polymer, or hydrolytic cleavage of the polyester backbone.

We have developed five polyester-based dynamic imine materials with varied cross-linking density and moderate renewable content. These materials exhibit high tensile strengths and can be reprocessed multiple times with full recovery of their thermomechanical properties. The structure of the pre-polymer (gradient or statistical) dictates the physicochemical properties of the imine networks at elevated temperatures but does not significantly alter their tensile properties at service temperatures. While we present evidence that imine exchange occurs primarily via an associative pathway in these networks, imine dissociation can be triggered under mildly acidic conditions to recover linear pre-polymer. Therefore, these dynamic imine networks synthesized from ROCOP pre-polymers exhibit valuable material properties while offering improved sustainability through partial bio-sourcing, continued reprocessing, and triggered degradation.

Results and Discussion

Polyester Network Synthesis

Tuning the ratio of aldehyde-containing **VG** and the epoxide co-monomer (**PO** or **GG**) enables us to control the cross-linking density of the resultant network. We prepared three terpolymers with 62%, 42%, and 23% **PO** incorporation relative to **PA** (**PO$_{x\%}$-*grad*** series). We found that these pre-polymers exhibited a gradient structure as a consequence of the high polymerisation temperature (80 °C) forcing volatile **PO** into the headspace (*vide infra*). We therefore reduced the reaction temperature and volume to synthesize a statistical analogue (**PO$_{35\%}$-*stat***) to directly compare the effect of pre-polymer architecture on the ultimate network properties. Our renewable network, **GG$_{43\%}$-*stat***, has a similar **VG** content and statistical pre-polymer architecture to **PO$_{35\%}$-*stat***.

The alternating ring-opening terpolymerisation of **PA** and **VG** with either **PO** or **GG** was catalysed by a bifunctional aluminium complex.[80] We targeted low molar mass materials (3–6 kDa) to exclude the effects of backbone entanglement on the observed properties of the final networks.[81,82] The pre-polymers contain 7–11 aldehydes per chain and exhibit glass transition temperatures (T_g) between 49–71 °C (Table 1). As in most ROCOP systems, the molar mass distributions exhibited moderate bimodality due to the presence of both catalyst-derived monofunctional initiators and adventitious bifunctional initiators (i.e. water, diol, or diacid) (Figure S2). Multimodal molecular weight distributions can significantly alter properties of linear materials,[83–85] but we anticipated that this effect would be mitigated upon cross-linking to form an infinite network.

A liquid diamine, 2,2'-(ethylenedioxy)bis(ethylamine), was selected as a cross-linker due to its miscibility with pre-polymer in solution. An amine:aldehyde ratio of 0.98:1 was used to promote high amine consumption, minimizing the amount of residual free amine that could react with the polyester backbone (*vide infra*). Pre-polymer and diamine were combined in THF, and this mixture gelled within 5 minutes. Slow evaporation of the solvent over several hours facilitated the formation of homogeneous materials. The networks were cured at 100 °C under dynamic vacuum for 12 hours to remove water from the system and thus drive the aldehyde/imine equilibrium towards imine formation.

Once cured, the networks were processed in a hot press at 90 or 100 °C for 30 minutes to produce smooth, homogenous, clear yellow films (Figure 1) that could be used for tensile and dynamic mechanical testing. FT-IR confirmed high conversion of aldehyde and amine to imine. In all cases, the spectra showed the disappearance of the aldehyde C=O (1681 cm^{-1}) and amine N–H (3375 cm^{-1}) stretching peaks, as well as the appearance of an imine C=N (1642 cm^{-1}) stretching frequency (Figure 1, Figures S1 and S36–S40). The films demonstrated gel fractions in THF that were quantitative or nearly so (≥ 94%) for four of the five networks (Table S5). Notably, the network with the lowest targeted cross-linking density, **PO$_{62\%}$-*grad*** had a relatively low gel fraction of 76%. While Flory-Stockmayer gel point calculations support sufficient cross-linking to form an infinite percolating network, some amount of unincorporated chains apparently remains.[86,87]

To study possible polyester cleavage and irreversible amide formation, **pre-PO$_{62\%}$-*grad*** and aldehyde-free **PA-*alt*-PO** polyester were separately reacted with *n*-hexylamine and subjected to curing conditions. In both cases, the absence of amide peaks in the ^{1}H and ^{13}C NMR spectra and minimal tailing in the GPC traces suggest that amidation was negligible under these conditions (Figures S6–S11). Nevertheless, we avoided prolonged heating of the networks above 100 °C to minimize any undesirable amidation. The cross-linked materials maintained their tensile and rheological properties over multiple reprocessing cycles (*vide infra)*, and no chemical changes were observed by infrared spectroscopy (FT-IR, Figures S36–S40), further indicating that irreversible amidation was avoided.

Table 1 Pre-polymer and pristine network properties

Network	$T_{g,\ pre\text{-}polymer}$ (°C) [a]	$T_{g,\ network}$ (°C) [a]	$T_{g,\ network}$ (°C) [b]	$T_{d,5\%}$ (°C) [c]	$M_{x,eff}$ (g/mol) [d]	σ_B (MPa) [e]	ε_B (%) [e]	E (GPa) [f]
$PO_{62\%}$-*grad*	47	64	65	318	331	60 ± 4	3.7 ± 0.5	2.1 ± 0.1
$PO_{42\%}$-*grad*	52	67	76	306	219	77 ± 4	5.7 ± 0.9	2.1 ± 0.1
PO_{23}			85					

Polyester Imine Network Properties

The thermal and mechanical properties of the cross-linked networks were characterized (Table 1). Differential scanning calorimetry (DSC) showed that the T_g values of all networks were well-above room temperature (57–69 °C) (Table 1). As the **PO** content decreased and cross-linking density increased in the **$PO_{x\%}$-*grad*** series, the T_g values increased (Table 1). Tensile testing revealed the strong, brittle nature of the films, similar to the tensile behaviour of typical thermoset resins. The stresses at break were near 70 MPa for all materials, indicating that tensile strengths at room temperature were independent of cross-linking density or comonomer composition (Table 1, Figures S31–S35).

Changes in network properties due to cross-linking density were observed using dynamic mechanical thermal analysis (DMTA) (Figure 2). As expected, increasing **VG** content in the **$PO_{x\%}$-*grad*** materials resulted in increasing storage moduli at elevated temperatures. The calculated molar mass between cross-links ($M_{x,eff}$) increased from 117 to 219 to 292 g/mol as the **VG** content decreased from 77% (**$PO_{23\%}$-*grad***) to 58% (**$PO_{42\%}$-*grad***) to 38% (**$PO_{62\%}$-*grad***) (Equation S1), further verifying the modularity and efficient curing of these networks. The calculated $M_{x,eff}$ values for **$PO_{35\%}$-*stat*** and **$GG_{43\%}$-*stat*** were comparable at 142 and 144 g/mol, respectively.

DMTA profiles can be used as evidence for associative versus dissociative exchange mechanisms within CANs. An extended rubbery plateau above the T_g is characteristic of a constant cross-linking density and is therefore expected for networks undergoing associative exchange reactions. By contrast, decreasing modulus—and thus decreasing cross-linking density—at elevated temperatures can be attributed to bond dissociation on timescales faster than the measurement.[16] Because each network contains the same dynamic functionality, we anticipated similar DMTA profiles for all materials; however, we observed two distinct behaviours (Figure 2). Both **$PO_{35\%}$-*stat*** and **$GG_{43\%}$-*stat*** exhibit an extended rubbery plateau past 70 °C, consistent with an associative mechanism. By contrast, the **$PO_{x\%}$-*grad*** networks exhibit an abridged plateau before their moduli begin to decrease at elevated temperatures. In fact, the viscosity at elevated temperature was so low that the sample length extended by up to 300% during DMTA (Figures S12–S16 and S27). We hypothesized the decreasing moduli and elongation of the **$PO_{x\%}$-*grad*** materials could be attributed to either dissociative imine exchange or thermomechanical effects related to polymer architecture.

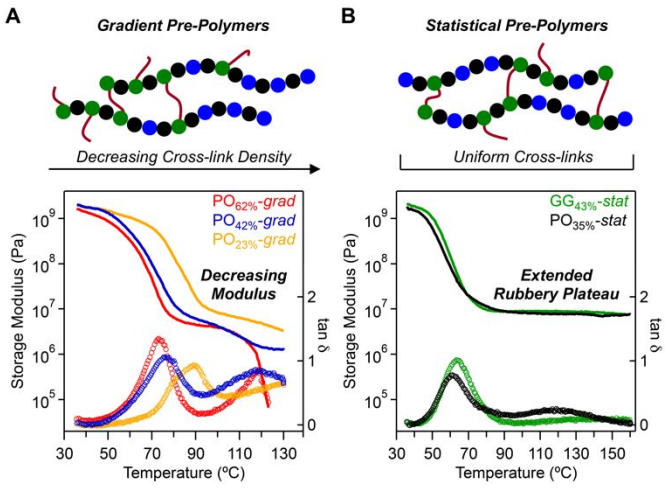

Fig 2 DMTA of imine exchange CANs derived from gradient (**A**) and statistical (**B**) pre-polymers. Networks from gradient pre-polymers show a decreasing modulus at elevated temperature because the networks are plasticized by lightly cross-linked polymer tails, greatly decreasing the viscosity of the materials. Networks from statistical pre-polymers exhibit extended rubbery plateaus due to their uniform cross-links.

In 2017, Rowan and co-workers studied the effects of dissociation rate on the rheological properties of a series of *N*-alkyl-substituted poly(alkylurea-urethanes).[16] The authors observed that the rubbery modulus remained constant while the bond equilibrium was shifted towards associated ureas. However, at a critical temperature (T_{flow}), dissociative processes dominated and caused the plateau modulus to drop as the cross-linking density decreased. As previously demonstrated, imine exchange can operate through dissociative mechanisms that are thermally activated or water catalysed.[40,41] For our materials, it is unlikely that changing the pre-polymer composition or architecture would alter the reaction mechanism between **VG** and the diamine cross-linker, particularly since each epoxide unit is effectively isolated by alternation with **PA**. Furthermore, elevated temperature solvolysis experiments revealed that the networks do not dissolve in pH neutral solvents, even above the T_g at 120 °C. This solvent resistance is strong evidence that a dissociative mechanism is not operative (*vide infra*, Figure S57). Thus, we do not believe the **$PO_{x\%}$-*grad*** networks' decreasing moduli can be attributed to cross-link dissociation.

As previously discussed, several reports have identified cross-link distribution and pre-polymer architecture as factors that influence the rheological properties of CANs.[45–47] Inspired by these reports, we suspected that the observed differences in DMTA were related to differences in pre-polymer architecture that arose during ROCOP of **GG** or **PO** epoxide comonomers with **VG** and **PA**. Due to their structural

similarity, **VG** and **GG** are expected to exhibit similar reactivity and thus yield a statistical terpolymer. **PO** and **VG**, however, differ in steric hindrance and electronic activation, which may lead to different rates of incorporation and yield blocky or gradient structures. For example, Zhang and co-workers reported different comonomer reactivities of glycidyl ethers and alkyl-substituted epoxides with **PA** in phosphazene base-catalysed ROCOP.[88] To assess the relative reactivities of **VG** and **PO**, **VG** incorporation was monitored over time in model ROCOPs with **PA** and either **PO** or **GG** (Figure S3). Using a 50:50 **VG**:**GG** feed ratio, we observed that **GG** and **VG** were indeed incorporated at similar rates throughout the polymerisation with **PA** to afford a statistical terpolymer. In analogous polymerisations with **PO** and **PA**, **VG** is preferentially—but not selectively—incorporated early in the polymerisation, producing a compositional gradient from 67:33 to 49:51 **VG**:**PO** (Figure S3). Aliquots taken during the syntheses of the **pre-PO$_{x\%}$-*grad*** series corroborate this gradient, rather than blocky, architecture (Table S4).

We therefore sought to synthesize an analogue to **PO$_{42\%}$-*grad*** with uniformly distributed cross-links. While the **PO$_{x\%}$-*grad*** pre-polymer series was synthesized at 80 °C to accelerate polymerisation, we recognized that volatile **PO** in the headspace of the reaction vessel could exacerbate tapering. To favour statistical incorporation of the epoxide comonomers, we reduced the reaction temperature and minimized the reaction volume. Aliquots from this reaction showed a more statistical incorporation of **VG**: at 30% conversion, the new material incorporated 72:28 **VG**:**PO**, which decreased only slightly to 65:35 **VG**:**PO** by the end of the reaction period. Gratifyingly, both networks from statistical pre-polymers (**PO$_{35\%}$-*stat*** and **GG$_{43\%}$-*stat***) showed an extended linear plateau, while all three networks from gradient terpolymers (**PO$_{x\%}$-*grad*** series) showed decreasing moduli at elevated temperatures (Figure 2). We are therefore confident the gradient versus statistical pre-polymer structures give rise to the observed differences by DMTA at elevated temperatures.

Gradient **VG** incorporation impacts the uniformity of cross-links within the network, which is known to have dramatic effects on the mechanical properties of both dynamic[45–47,89–91] and permanently cross-linked materials.[92–96] Notably, Li and co-workers modelled permanently cross-linked networks with aggregated or dispersed cross-links and found that the storage modulus decreased with less uniformly distributed cross-links.[96] Therefore, we propose that the inhomogeneity of cross-linking in the **PO$_{x\%}$-*grad*** networks causes their rapid flow and decreasing moduli at elevated temperatures. Previous studies of cross-linked networks have demonstrated that pendant chains serve as plasticizers that dissipate energy through viscoelastic relaxation processes.[92–95] We suspect that under tension at high temperatures, lightly (or even un-) cross-linked polymer tails may slide past each other, causing flow. **PO$_{62\%}$-*grad***, which has the lowest number of cross-links, exhibits the sharpest decrease in storage modulus during DMTA. Increasing the cross-linking density in the gradient materials (i.e. by increasing **VG** content) results in more gradual decreases in moduli. In the future, we believe pre-polymer structure and network homogeneity should be considered when assessing the thermomechanical behaviours of dynamic networks.

Dynamic Exchange Mechanism

Fast imine exchange in the networks was observed using stress relaxation analysis (SRA). An instantaneous shear strain was applied at a given temperature, and the exponential decay of the resultant stress was measured over time. Characteristic relaxation times (τ^*) were determined when the stress reached 37% ($^1/_e$) of its initial value. The rapid flow of the **PO$_{x\%}$-*grad*** series (*vide supra*) prohibited accurate measurements of relaxation time in a parallel plate geometry. **GG$_{43\%}$-*stat***, which showed an extended rubbery plateau, was therefore selected as a representative sample for SRA. This network exhibited remarkably fast relaxation rates, with τ^* values between 1 and 10 seconds at 105 to 120 °C. For exchange processes at a given temperature well above the network T_g, the observed relaxation rates typically depend only upon the energy required for chemical exchange.[5] Therefore, τ^* can be used as a representative rate to determine the Arrhenius temperature dependence of bond exchange in a network. Below 105 °C, **GG$_{43\%}$-*stat*** was too close to its T_g to exhibit classic exponential decay (Figure S29). Above 120 °C, the stress relaxation was so rapid (τ^* = 1.5 s) that reduced instrument resolution resulted in large errors across multiple runs. Therefore, values of τ^* were measured between 105–120 °C, and the resulting Arrhenius activation energy (E_a) for **GG$_{43\%}$-*stat*** was 69.5 ± 4.3 kJ/mol.

In CANs, the Arrhenius activation energy and pre-factor τ_0 can be used to determine the topological freezing temperature (T_v) at which bond exchange is sufficiently fast to rearrange network topology (Equations S2 and S3).[5,12] The theoretical T_v of **GG$_{43\%}$-*stat*** is –22 °C, which is well below its T_g value. This calculated value implies that at service temperatures, bond

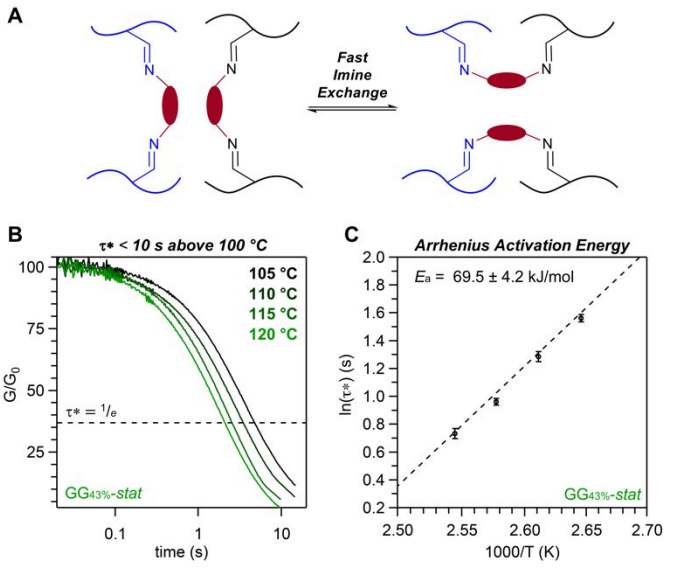

Fig 3 Representation of dynamic imine exchange in a cross-linked network (**A**). Stress relaxation analysis of **GG$_{43\%}$-*stat*** shows τ^* values less than 10 s at temperatures above 105 °C (**B**). The Arrhenius activation energy of 69.5 ± 4.2 kJ/mol for **GG$_{43\%}$-*stat*** was determined using stress relaxation rates from 105–120 °C (**C**).

exchange is frozen not by imine exchange kinetics, but by the lack of chain mobility. As the network is heated above its T_g, reorganisation is initially diffusion-controlled until sufficient thermal energy enables facile motion and Arrhenius exchange.[6,18]

The fast relaxation dynamics of the cross-linked networks prompted us to explore the mechanism of exchange. Imines are known to exchange by dissociative processes (hydrolysis) and/or associative processes (transimination with a primary amine or imine metathesis).[43,44] The polyester imine networks are cured at 100 °C (well above T_g) under dynamic vacuum, and thus there should be minimal residual water to catalyse the dissociative pathway. Additionally, Chao *et al.* demonstrated through small molecule models that hydrolysis was significantly slower than amine-catalysed transimination: 1.2 equivalents of water relative to imine were required to approach the rate obtained with 0.1 mol% of primary amine.[33]

We therefore sought to distinguish between the two possible associative mechanisms by monitoring imine exchange in small molecule models by ^{1}H NMR spectroscopy. Because of the rapid reaction in solution, kinetics experiments were conducted below 0 °C. Mixing equimolar amounts of model two imine compounds in CD_3CN at –20 °C afforded little conversion to their cross-products over the reaction period (Figure S51). Warming the reaction to ambient temperature produced no further conversion. However, addition of a catalytic amount of neopentyl amine yielded a statistical distribution of imine products even at low temperatures (Figures S51 and S52). The rate of imine metathesis is therefore negligible relative to that of amine-catalysed transimination in this model system. Monitoring the reaction progress over –30 to –5 °C afforded rate constants k_{obs} that were used to calculate an Arrhenius activation energy of 36.5 ± 2.1 kJ/mol for amine-catalysed transimination (Table S12 and Figure S53).

The large discrepancy between the small molecule model and the network E_a values warrants a more detailed mechanistic analysis that is beyond the scope of this study.[7,11] Low soluble fractions suggest there is minimal unreacted amine present in the networks. However, limited mobility of these moieties could restrict amine-catalysed transimination. Previous CANs have demonstrated Arrhenius activation energies which match or surpass those of small molecule models; any discrepancies are typically attributed to the energetic requirements of polymer segmental motion.[97,98]

As a complementary approach, common laboratory solvents were screened in order to identify conditions under which the networks dissociated (Figures S54 and S55). The materials swelled in water, dichloromethane, and tetrahydrofuran and exhibited no significant changes in acetone, ethyl acetate, toluene, and hexanes; in these solvents, the networks remained intact when submerged over multiple days. Importantly, the networks also did not dissolve when heated above the T_g to 120 °C in 1,4-dioxane, which readily solubilizes pre-polymer (Figure S57). This solvent resistance suggests that imine exchange in these networks is primarily achieved via an associative mechanism, as dissociative exchange would result in dissolution. Notably, chloroform dissolved representative networks **PO$_{35\%}$-*stat*** and **GG$_{43\%}$-*stat*** in under six hours. This dissolution in chloroform, but not DCM or water, suggests an acid-catalysed process given trace acid typically found in chloroform. When submerged in a 5% solution of triethylamine and chloroform, the networks swelled but did not dissolve (Figure S56).

Vitrimer-Like Reprocessing

CANs represent a notable improvement over permanently cross-linked materials due to their reprocessability. To demonstrate this key attribute, we ground each of the imine cross-linked polyester networks into ~1 mm wide granules and reprocessed the materials over several cycles in a hot press (Figures S12–S20). After each cycle, the materials were analysed by DMTA and uniaxial elongation experiments to assess the cross-linking density and the tensile strength recovery, respectively.

Reprocessing conditions were optimized over three cycles using **GG$_{43\%}$-*stat*** (Figure 4). The first cycle (90 °C, 5 minutes) yielded visually homogeneous dogbones with near quantitative recovery of cross-linking density by DMTA. However, the stress at break was significantly lower (~50%) relative to the pristine material. Although the materials were visually indistinguishable and cross-linking density remained unchanged throughout the reprocessing cycles, the tensile behaviour suggests that the material was not fully fused and likely contained microscopic cracks that caused premature fracture at relatively low stress. The reprocessing time and temperature were increased for the second cycle (100 °C, 15 minutes), which significantly improved tensile strength recovery (~80%). Finally, extending the processing time (100 °C, 30 minutes) afforded identical films with near quantitative recovery of tensile strength and cross-linking density.

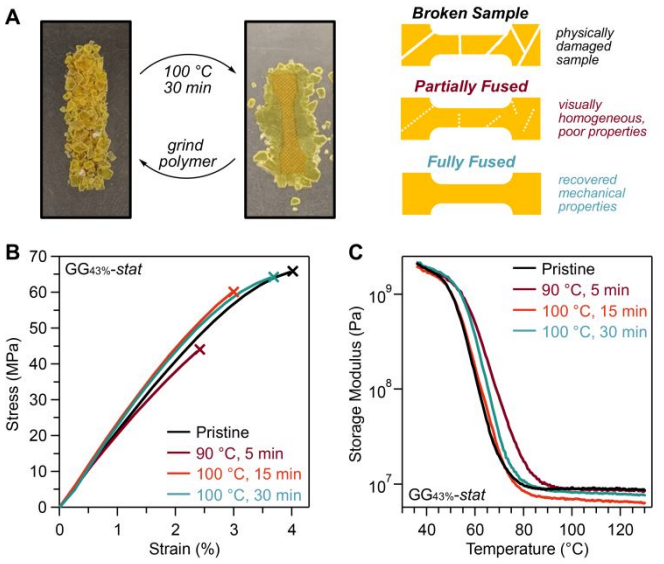

Fig 4 Imine-exchange CANs were repeatedly ground into granules and pressed in a hot press to reform homogenous, cross-linked networks. Particulates must have sufficient time to flow together and fully fuse in order to recover mechanical properties (**A**). The optimized reprocessing procedure for representative **GG$_{43\%}$-*stat*** shows full recovery of tensile properties (**B**) and cross-linking density (**C**) after three reprocessing cycles.

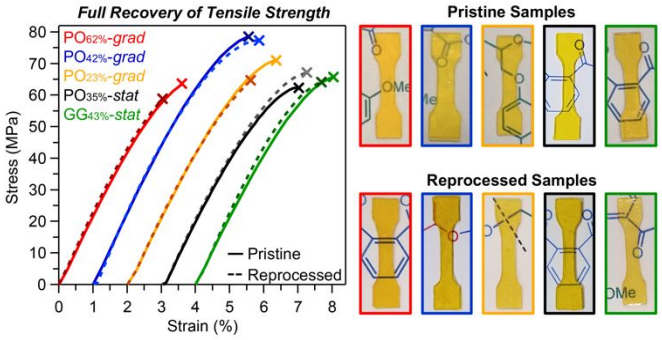

Fig 5 Optimized reprocessing procedures give quantitative recovery of tensile properties for all five networks after three reprocessing cycles (left). Tensile testing traces are horizontally offset from the origin in increments of 1% strain for clarity. The networks are visually homogeneous and unchanged after three reprocessing cycles (right).

Therefore, it is important to consider not only the rate at which the dynamic bonds exchange, but also the macroscopic flow rate required for a material to fuse.

The optimized reprocessing procedure provided full recovery of tensile strength and cross-linking density for all five networks (Figure 5, Figures S22–26 and S31–35). The pristine and reprocessed materials were all identical in appearance (Figure 5), and no chemical changes were observed via FT-IR spectroscopy (Figures S36–S40). Additionally, these polyester imine materials are stable over multiple cycles and require relatively short reprocessing times at moderate temperatures.

Alternative End-of-Life Fates

While imine-based CANs likely rely on an associative mechanism in bulk networks, dissociation can be triggered under aqueous or acidic conditions to regenerate the starting materials.[66,68,70] Based on our solvolysis experiments, we anticipated that dissolution of the polyester imine networks in mildly acidic environments would enable pre-polymer recovery. ^{1}H NMR spectroscopy of the **PO$_{35\%}$-*stat*** dissolution products in $CDCl_3$ revealed a ~93:7 ratio of imine:aldehyde (Figure S58), suggesting some intramolecular loops or pre-polymer dimers and trimers remain. Addition of two equivalents of HCl (12 M) with respect to **VG** resulted in nearly quantitative dissociation by ^{1}H NMR spectroscopy (Figure S58). Upon scaling up, pre-polymer could be recovered in 91% yield after precipitation into methanol. The ^{1}H and ^{13}C NMR spectra of the recovered material were consistent with those of pristine **PO$_{35\%}$-*stat*** (Figures S60 and S61). However, the GPC trace of the recovered polymer revealed a slight increase in both peak molecular weight and the amount of high molecular weight components, consistent with a small amount of pendant amine and dimerisation, respectively (Figure S62). This recovery strategy represents an orthogonal recycling approach to network reprocessing. Alternatively, polyester backbones may be hydrolytically degraded under acidic, basic, or enzymatic conditions.[59–63]

Conclusions

The ring-opening copolymerisation of epoxides and cyclic anhydrides provides a modular platform to synthesize polyester pre-polymers with varied architectures. Cross-linking these linear polyesters with a flexible diamine affords reprocessable thermoset materials with high tensile strengths and solvent resistance. Although the networks demonstrate similar mechanical properties at service temperatures, pre-polymer composition and structure significantly influence their rheological behaviour at elevated temperatures: statistical pre-polymers afford an extended rubbery plateau modulus, whereas gradient pre-polymer architectures produce an abridged plateau followed by flow. Stress relaxation analysis reveals rapid imine dynamics, and a solvolysis study suggests associative exchange mechanisms (transimination or metathesis) predominate in the networks. The polyester imine materials exhibit quantitative recovery of tensile properties and cross-linking density over multiple reprocessing cycles. Triggered dissociation to pre-polymer and hydrolytic cleavage of the polyester backbone provide additional end-of-life alternatives to thermal recycling.

We believe the modular ROCOP approach provides a flexible platform to probe the relationship between CAN architecture and observed dynamics. In the future, this synthetic strategy could permit facile variation of the relative ratio of permanent and dynamic crosslinks in dynamic networks, exploration of blocky, gradient, and statistical backbone effects, or comparison of different dynamic chemistries within the same polymer backbone.

Conflicts of interest

There are no conflicts to declare.

Acknowledgements

We thank Stephanie Liffland for performing DMTA analyses of several materials. This research was supported by the Center for Sustainable Polymers — a National Science Foundation Center for Chemical Innovation (CHE-1901635), the University of Minnesota, and Cornell University. C.A.L.L. gratefully acknowledges a graduate research fellowship from the National Science Foundation (DGE-1650441). G.X.D. gratefully acknowledges a University of Minnesota doctoral dissertation fellowship. This work made use of the Cornell Center for Materials Research and the NMR Facility at Cornell University, which are supported by the NSF under awards DMR-1719875 and CHE-1531632, respectively.

Notes and references

1 D. K. Schneiderman and M. A. Hillmyer, *Macromolecules*, 2017, **50**, 3733–3749.
2 M. Hong and E. X.-Y. Chen, *Green Chem.*, 2017, **19**, 3692–3706.
3 W. Zou, J. Dong, Y. Luo, Q. Zhao and T. Xie, *Adv. Mater.*, 2017, **29**, 1606100.

4 D. J. Fortman, J. P. Brutman, G. X. De Hoe, R. L. Snyder, W. R. Dichtel and M. A. Hillmyer, *ACS Sustainable Chem. Eng.,* 2018, **6**, 11145–11159.
5 Z. P. Zhang, M. Z. Rong, M. Q. Zhang, *Prog. Polym. Sci.,* 2018, **80**, 39–93.
6 W. Denissen, J. M. Winne and F. E. Du Prez, *Chem. Sci.,* 2016, **7**, 30–38.
7 G. M. Scheutz, J. J. Lessard, M. B. Sims and B. S. Sumerlin, *J. Am. Chem. Soc.,* 2019, **141**, 16181–16196.
8 P. Chakma and D. Konkolewicz, *Angew. Chem., Int. Ed.*, 2019, **58**, 9682–9695.
9 L. Imbernon and S. Norzez, *Eur. Polym. J.,* 2016, **82**, 347–376.
10 C. J. Kloxin and C. N. Bowman, *Chem. Soc. Rev.*, 2013, **42**, 7161–7173.
11 J. M. Winne, L. Leibler and F. E. Du Prez, *Polym. Chem.*, 2019, **10**, 6091–6108.
12 D. Montarnal, M. Capelot, F. Tournilhac and L. Leibler, *Science*, 2011, **334**, 965–968.
13 E. Chabert, J. Vial, J. Cauchois, M. Mibaulta and F. Tournilhac, *Soft Matter*, 2016, **12**, 4838–4845.
14 Q. Shi, K. Yu, X. Kuang, X. Mu, C. K. Dunn, M. L. Dunn, T. Wang and H. J. Qi, *Materials Horizons,* 2014, **4**, 598–607.
15 X. Chen, M. A. Dam, K. Ono, A. Mal, H. Shen, S. R. Nutt, K. Sheran and F. Wudl, *Science*, 2002, **295**, 1698–1702.
16 L. Zhang and S. J. Rowan, *Macromolecules*, 2017, **50**, 5051–5060.
17 D. J. Fortman, J. P. Brutman, C. J. Cramer, M. A. Hillmyer and W. R. Dichtel, *J. Am. Chem. Soc.*, 2015, **137**, 14019–14022.
18 M. Capelot, M. M. Unterlass, F. Tournilhac and L. Leibler, *ACS Macro. Lett.,* 2012, **1**, 789–792.
19 M. Delahaye, J. M. Winne and F. E. Du Prez, *J. Am. Chem. Soc.*, 2019, **141**, 15277–15287.
20 W. Denissen, M. Droebeke, R. Nicolaÿ, L. Leibler, J. M. Winne and F. E. Du Prez, *Adv. Funct. Mater.,* 2015, **25**, 2451–2457.
21 W. Denissen, M. Droebeke, R. Nicolaÿ, L. Leibler, J. M. Winne and F. E. Du Prez, *Nat. Commun.,* 2017, **8**, 14857.
22 J. J. Lessard, L. F. Garcia, C. P. Easterling, M. B. Sims, K. C. Bentz, S. Arencibia, D. A. Savin and B. S. Sumerlin, *Macromolecules,* 2019, **52**, 2105–2111.
23 W. Denissen, I. De Baere, W. Van Paepegem, L. Leibler, J. Winne and F. E. Du Prez, *Macromolecules,* 2018, **51**, 2054–2064.
24 J. S. A. Ishibashi and J. A. Kalow, *ACS Macro. Lett.*, 2018, **7**, 482–486.
25 A. Ruiz de Luzuriaga, R. Martin, N. Markaide, A. Rekondo, G. Cabañero, J. Rodríguez and I. Odriozola, *Mater. Horiz.,* 2016, **3**, 241–247.
26 A. Takahashi, R. Goseki, K. Ito and H. Otsuka, *ACS Macro. Lett.,* 2017, **6**, 1280–1284.
27 B. T. Michael, C. A. Jaye, E. J. Spencer and S. J. Rowan, *ACS Macro. Lett.*, 2013, **2**, 694 – 699.
28 P. Zheng and T. J. McCarthy, *J. Am. Chem. Soc.,* 2012, **134**, 2024–2027.
29 Y. Nishimura, J. Chung, H. Muradyan and Z. Guan, *J. Am. Chem. Soc.*, 2017, **139**, 14881–14884.
30 M. Röttger, T. Domenech, R. van der Weegen, A. Breuillac, R. Nicolaÿ and L. Leibler, *Science*, 2017, **356**, 62–65.
31 J. C. Lai, J. F. Mei, X. Y. Jia, C. H. Li, X. Z. You and Z. A. Bao, *Adv. Mater.*, 2016, **28**, 8277–8282.
32 H. Li, J. Bai, Z. Shi and J. Yin, *Polymer*, 2016, **85**, 106–113.
33 A. Chao, I. Negulescu and D. Zhang, *Macromolecules,* 2016, **49**, 6277–6284.
34 M. Kathan, P. Kovaříček, C. Jurissek, A. Senf, A. Dallmann, A. F. Thünemann and S. Hecht, *Angew. Chem., Int. Ed.*, 2016, **55**, 13882–13886.
35 X. Lei, Y. Jin, H. Sun and W. Zhang, *J. Mater. Chem. A,* 2017, **5**, 21140–21145.
36 R. Mo, J. Hu, H. Huang, Z. Sheng and X. Zhang, *J. Mater. Chem. A,* 2019, **7**, 3031–3038.
37 C. Zhu, C. Xi, W. Doro, T. Wang, X. Zhang, W. Jin and W. Zhang, *RSC Adv.,* 2017, **7**, 48303–48307.
38 P. Taynton, K. Yu, R. K. Shoemaker, Y. Jun, H. J. Qi and W. Zhang, *Adv. Mater.*, 2014, **26**, 3938–3942.
39 P. Taynton, H. Ni, C. Zhu, K. Yu, S. Loob, Y. Jin, H. J. Qi and W. Zhang, *Adv. Mater.,* 2016, **28**, 2904–2909.
40 P. Taynton, C. Zhu, S. Loob, R. Shoemaker, K. Pritchard, Y. Jin and W. Zhang, *Polym. Chem.,* 2016, **7**, 7052–7056.
41 F. Song, Z. Li, P. Jia, M. Zhang, C. Bo, G. Feng, L. Hu and Y. Zhou, *J. Mater. Chem. A,* 2019, **7**, 13400–13410.
42 Y. Liu, Z. Tang, J. Chen, J. Xiong, D. Wang, S. Wang, S. Wu and B. Guo, *Polym. Chem.,* 2020, DOI: 10.1039/C9PY01826C.
43 M. E. Belowich and J. F. Stoddart, *Chem. Soc. Rev.,* 2012, **41**, 2003–2024.
44 M. Ciaccia and S. Di Stefano, *Org. Biomol. Chem.,* 2015, **13**, 646–654.
45 J. Ishibashi, Y. Fang, J. Kalow, *ChemRxiv*, 2019, Preprint, DOI:10.26434/chemrxiv.10000232
46 J. J. Lessard, G. M. Scheutz, S. H. Sung, K. A. Lantz, T. H. Epps III, B. S. Sumerlin. *J. Am. Chem. Soc.*, 2020, **142**, 283–289.
47 R. G. Ricarte, F. Tournilhac and L. Leibler, *Macromolecules*, 2019, **52**, 432–443.
48 S. Paul, Y. Zhu, C. Roman, R. Brooks, P. K. Saini and C. K. Williams, *Chem. Comm.*, 2015, **51**, 6459–6479.
49 J. M. Longo, M. J. Sanford and G. W. Coates, *Chem. Rev.*, 2016, **116**, 15167–15197.
50 N. J. Van Zee and G. W. Coates, *Angew. Chem., Int. Ed.*, 2015, **54**, 2665–2668.
51 M. J. Sanford, L. Pena Carrodeguas, N. J. Van Zee, A. W. Kleij and G. W. Coates, *Macromolecules*, 2016, **49**, 6394–6400.
52 P. K. Saini, C. Romain, Y. Zhu and C. K. Williams, *Polym. Chem.,* 2014, **5**, 6068–6075.
53 A. Thevenon, J. A. Garden, A. J. P. White and C. K. Williams, *Inorg. Chem.,* 2015, **54**, 11906–11915.
54 M. Winkler, C. Romain, M. A. R. Meier and C. K. Williams, *Green Chem.,* 2015, **17**, 300–306.
55 Y. Zhu, C. Romain and C. K. Williams, *J. Am. Chem. Soc.,* 2015, **137**, 12179–12182.
56 J. Y. Jeon, S. E. Chan, J. K. Varghese and B. Y. Lee, *Beilstein J. Org. Chem.,* 2014, **10,** 1787–1795.
57 R. Mundil, Z. Hošťálek, I. Šeděnková and J. Merna, *Macromol. Res.,* 2015, **23**, 161–166.
58 M. J. Sanford, N. J. Van Zee and G. W. Coates, *Chem. Sci.*, 2018, **9**, 134–142.
59 M. Vert, *Biomacromolecules,* 2005, **6**, 538–546.
60 D. A. Olson, S. E. A. Gratton, J. M. DiSimone and V. V. Sheares, *J. Am. Chem. Soc.* 2006, **128**, 13625–13633.
61 R.-J. Müller, I. Kleeberg and W.-D. Deckwer, *J. Biotechnol.,* 2001, **86**, 87–95.
62 A. H. Brown and V. V. Sheares, *Macromolecules,* 2007, **40**, 4848–4853.
63 G. X. De Hoe, M. T. Zumstein, B. J. Tiegs, J. P. Brutman, K. McNeill, M. Sander, G. W. Coates and M. A. Hillmyer, *J. Am. Chem. Soc.,* 2018, **140**, 963−973.

64 X. Yu, J. Jia, S. Xu, K. U. Lao, M. J. Sanford, R. K. Ramakrishnan, S. I. Nazarenko, T. R. Hoye, G. W. Coates and R. A. DiStasio, *Nat. Commun.,* 2018, **9**, 2880–2888.
65 M. Fache, B. Boutevin and S. Caillol, *Green Chem.*, 2016, **18**, 712–725.
66 S. Wang, S. Ma, Q. Li, W. Yuan, B. Wang and J. Zhu, *Macromolecules*, 2018, **51**, 8001–8012.
67 S. Zhao and M. M. Abu-Omar, *Macromolecules*, 2018, **51**, 9816–9824.
68 H. Geng, Y. Wang, Q. Yu, S. Gu, Y. Zhou, W. Xu, X. Zhang and D. Ye, *ACS Sustainable Chem. Eng.*, 2018, **6**, 15463–15470.
69 Q. Yu, X. Peng, Y. Wang, H. Geng, A. Xu, X. Zhang, W. Xu and D. Ye, *Eur. Polym. J.*, 2019, **117**, 55–63.
70 S. Wang, S. Ma, Q. Li, X. Xu, B. Wang, W. Yuan, S. Zhou, S. You and J. Zhu, *Green Chem.*, 2019, **21**, 1484–1497.
71 A. Llevot, E. Grau, S. Carlotti, S. Grelier and H. Cramail, *Macromol. Rapid Commun.*, 2016, **37**, 9–28.
72 M. Fache, E. Darroman, V. Besse, R. Auvergne, S. Caillol and B. Boutevin, *Green Chem.*, 2014, **16**, 1987–1998.
73 B. M. Bell, J. R. Briggs, R. M. Campbell, S. M. Chambers, P. D. Gaarenstroom, J. G. Hippler, B. D. Hook, K. Kearns, J. M. Kenney, W. J. Kruper, D. J. Schreck, C. N. Theriault and C. P. Wolfe, *Clean: Soil, Air, Water,* 2008, **36**, 657−661.
74 A. Sobrero, *Ann.*, 1843, **48**, 19.
75 H. F. Lewis and I. A. Pearl, *US Pat*., 2 433 227, 1944.
76 J. D. McGinness, J. A. Whittenbaugh and C. A. Lucchesi, *Tappi*, 1960, **43**, 1027–1029.
77 E. Mahmoud, D. A. Watson and R. F. Lobo, *Green Chem.*, 2014, **16**, 167–175.
78 C. E. Andrews, *US Pat.*, 1 336 182, 1920.
79 H. Baer, M. Bergamo, A. Forlin, L. H. Pottenger and J. Linder, in *Ullmann's Encyclopedia of Industrial Chemistry*, Wiley-VCH, Weinhein, 7th Edition, 2012, Propylene Oxide, 1–29.
80 B. A. Abel, C. A. L. Lidston and G. W. Coates, *J. Am. Chem. Soc.,* 2019, **141**, 12760–12769.
81 J. R. Dorgan and J. S. Williams, *J. Rheol.,* 1999, **43**, 1141–1155.
82 J. Bicerano, *Prediction of Polymer Properties*, Marcel Dekker Inc., New York, 3rd Edition, 2009.
83 D. T. Gentekos, R. J. Sifri and B. P. Fors, *Nat. Rev. Mater.,* 2019, **4**, 761–774.
84 R. W. Nunes, J. R. Martin and J. F. Johnson, *Polym. Eng. Sci.,* 1982, **4**, 205–228.
85 R. Whitfield, N. P. Truong, D. Messmer, K. Parkatzidis, M. Rolland and A. Anastasaki, *Chem. Sci.*, 2019, **10**, 8724–8734.
86 P. Flory, *J. Am. Chem. Soc.*, 1941, **63**, 3083–3090.
87 W. H. Stockmayer, *J. Chem. Phys.*, 1944, **12**, 125–131.
88 H. Li, H. Luo, J. Zhao and G. Zhang, *Macromolecules,* 2018, **51**, 2247–2257.
89 L. Imbernon, S. Norvez and L. Leibler, *Macromolecules*, 2016, **49**, 2172–2178.
90 K. Jin, L. Li and J. M. Torkelson, *Adv. Mater.*, 2016, **28**, 6746–6750.
91 D. Pratchayanan, J. Yang and C. L. Lewis, *J. Rheol.*, 2017, **61**, 1359–1367.
92 K. Urayama, T. Kawamura and S. Kohjiya, *Polymer*, 2009, **50**, 347–356.
93 H. Yamazaki, M. Takeda, Y. Kohno, H. Ando, K. Urayama and T. Takigawa, *Macromolecules*, 2011, **44**, 8829–8834.
94 W. Yu, M. Du, D. Zhang, Y. Lin and Q. Zheng, *Macromolecules*, 2013, **46**, 7341–7351.
95 L. E. Roth, D. C. Agudelo, J. A. Ressia, L. R. Gómez, E. M. Vallés, M. A. Villar and D. A. Vega, *Eur. Polym. J.*, 2015, **64**, 1–9.
96 J. Shen, X. Lin, J. Liu and X. Li. *Macromolecules*, 2019, **52**, 121–134.
97 R. L. Snyder, D. J. Fortman, G. X. De Hoe, M. A. Hillmyer and W. R. Dichtel, *Macromolecules*, 2018, **51**, 389–397.
98 K. Yu, P. Taynton, W. Zhang, M. L. Dunn, and H. J. Qi, *RSC Adv.,* 2014, **4**, 48682−48690.

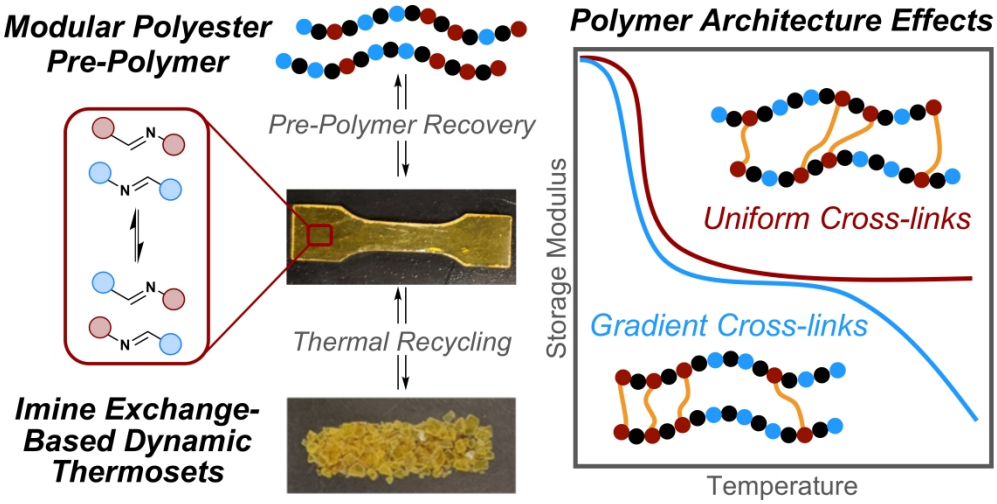
Modular Polyester Pre-Polymer
Pre-Polymer Recovery
Thermal Recycling
Imine Exchange-Based Dynamic Thermosets
Polymer Architecture Effects
Storage Modulus
Uniform Cross-links
Gradient Cross-links
Temperature